



Quantitative measurement of aggregation kinetics process of nanoparticles using nanoparticle tracking analysis and dynamic light scattering

Chao Wang · Bowen Lv · Jun Hou · Peifang Wang · Lingzhan Miao · Hanlin Ci

Received: 23 January 2019 / Accepted: 9 April 2019 / Published online: 24 April 2019
© Springer Nature B.V. 2019

Abstract The cerium dioxide nanoparticle (CeO₂ NP) (122 nm) aggregation process was investigated by nanoparticle tracking analysis (NTA), and the results were compared with those of dynamic light scattering (DLS). Unlike descriptions based on classical aggregation kinetics theory, the size distributions obtained by NTA and DLS show that aggregation of NPs in an aquatic environment is a complicated process and highly dependent on the particle number concentration, which is information that has been rarely presented in the literature. In particular, not all the particles were aggregated and there still remained some small CeO₂ NPs (< 400 nm), which has potential adverse environmental risks to the ecosystem and public health. Furthermore, the aggregate sizes are far smaller than previously shown in aggregation kinetics experiments. In addition, our findings also indicate that NTA can measure samples with mass concentrations ranging from 0.1 to 100 mg/L without dilution. In contrast, DLS cannot provide accurate information about aggregation kinetics when the mass concentration of CeO₂ NPs is lower than 1 mg/L ($2.02 \times 10^8 \pm 1.66 \times 10^7$ by NTA data). Consequently, the classical aggregation kinetics experiment using DLS cannot accurately reflect the fate of NPs in aquatic environment,

especially the heteroaggregation of NPs in complex water phase, and these results further demonstrate that the toxicity evaluation of NPs concerning different sizes measured by DLS need more rigorously experimental design. Therefore, our findings provide the first quantitative attempt to explore the experimental conditions and analytical methods for further study of aggregation kinetics.

Keywords CeO₂ nanoparticles · Aggregation kinetics · Nanoparticle tracking analysis · Dynamic light scattering

Introduction

As nanotechnology continues to rapidly develop, engineered nanomaterials (ENMs) are widely used in printers, cosmetics, electronics, catalysts, medicine, electronics, groundwater remediation, waste water treatment, and many other applications (Hou et al. 2015; Zhu et al. 2014). There are currently over 1000 ENM-enabled consumer products (Romerofranco et al. 2017), and between 100 and 1000 tons of cerium dioxide nanoparticles (CeO₂ NPs) can be produced each year

Electronic supplementary material The online version of this article (<https://doi.org/10.1007/s11051-019-4527-0>) contains supplementary material, which is available to authorized users.

C. Wang · B. Lv · J. Hou (✉) · P. Wang · L. Miao · H. Ci
Key Laboratory of Integrated Regulation and Resources
Development on Shallow Lakes of Ministry of Education, College
of Environment, Hohai University, Nanjing 210098, People's

Republic of China
e-mail: hhuhjyhj@126.com

by a single manufacturer (Piccinno et al. 2012). However, the rapid growth of the market for ENMs means that the release of NPs from manufactured ENMs is not well controlled, especially the discharge of NPs into aquatic system, resulting in severe water pollution (Bian et al. 2011; Li and Chen 2012). A clear understanding on the behavior (including aggregation, sedimentation, and dissolution) of NPs in water is therefore crucial to fully elucidate the life cycle and transport mechanisms of NPs in the environment and the subsequent ecosystem risk assessment.

Due to important environmental implication of NPs' aggregation rate (for example, affecting the rate of sedimentation and thus removal from an aquatic environment, and so on), several studies using dynamic light scattering (DLS) were conducted to investigate the aggregation kinetics of nanoparticles (NPs) under various conditions (Gallego-Urrea et al. 2016; Lee et al. 2015; Oriekhova and Stoll 2016; Praetorius et al. 2014). This set of methods has been proved to be feasible, and many meaningful results have been obtained (Li et al. 2017; Lin et al. 2016a; Sotirelis and Chrysikopoulos 2016; Xu et al. 2016). However, little attention has been given to whether DLS can reflect the actual state of NPs in experiments of aggregation kinetics since the results are usually overwhelmed by the contribution of a few large particles to overall scattering (Jiskoot and Crommelin 2005). As large particles scatter are much lighter than small particles, the scattering intensity of a particle is proportional to the sixth power of its diameter, leading to the failure of polydisperse solution detection and characterization (Filipe et al. 2010). Moreover, the particle concentration applied in these experiments is still controversial despite the clear relationship between the experimental value of particle concentration and the aggregation behavior. On one hand, according to the determination of aggregation kinetics, the hydrodynamic radius is linearly dependent on the initial particle concentration (Baalousha et al. 2013; Chen and Elimelech 2006; Chen et al. 2006; Loosli et al. 2015); on the other hand, owing to technical limitations, the experimental concentration is often higher than the estimated concentration in the environment. For instance, owing to their widespread use in commercial products, CeO₂ NPs are frequently chosen as the target NPs in studies on the environmental behavior of NPs in water (Hoecke et al. 2011; Keller et al. 2010; Li and Chen 2012; Quik et al. 2010). Data on the aggregation kinetics of CeO₂ NPs are summarized in Table S1, and the concentration of the NPs is typically in the range of 7.62–

55.00 mg/L. In order to obtain the optimum light-scattering intensity in DLS experiments, the CeO₂ concentration in many studies is higher than the expected concentration in the environment. However, little is known about the relationship between the experimental concentration and the experimental detection limits.

The nanoparticle tracking analysis (NTA), a laser-based, light-scattering system with an easy-to-use and reproducible platform, provides a direct, real-time visualization method for specific and general nanoparticle characterization (Dragovic et al. 2011a). The NTA system also tracks nanoparticles moving under Brownian motion and calculates their size and total concentration from the Stokes–Einstein equation (Dragovic et al. 2011b). Dragovic et al. reported that NTA can measure cellular vesicles as small as 50 nm since it is independent of the refractive index of the particle (Dragovic et al. 2011a). Elizabeth et al. (2014) investigated the transportation of TiO₂ NPs in various soil suspensions by NTA and reported that the higher stability of TiO₂ suspensions resulted in a higher mobility of TiO₂ through soil layers. Unlike DLS, NTA can track individual NPs and obtain more accurate particle-size distributions and concentrations. It was shown by Gillespie et al. (2011) that NTA can successfully monitor the growth of particles of a poorly water-soluble drug, which cannot be offered by DLS. Filipe et al. (2010) compared the performance of NTA and DLS in characterizing drug delivery nanoparticles and protein aggregates and the results suggested that NTA was more suitable than DLS for measuring polydisperse samples. However, few studies introduced NTA to explain the aggregation kinetics data obtained through DLS, while DLS alone may be insufficient for analyzing aggregation kinetics.

Despite its numerous advantages in several research areas, NTA has several limitations, including the small detection ranges of the sample particle concentration and particle size. NTA can only track individual particles within the range of 10–1000 nm and the concentration is acceptable between 10⁷ and 10⁹ total particles/mL (Griffiths et al. 2011; Filipe et al. 2010; Lungu et al. 2015). Furthermore, NTA software involves several settings that affect the accuracy of the measurement results. Operators can intentionally ignore or emphasize the presence of certain particles, which makes the results dependent on individual judgment and experience. Van der Pol et al. have shown how NTA distinguished silica and polystyrene beads based on their refractive index (Pol et al. 2014). In addition, Mehrabi et al. (2017) reported that due to the different refractivity index, the camera level

can be adjusted so “dark” that only the brighter, engineered particles can be tracked in natural solution. Therefore, NTA experimental results strongly depend on the operator and software parameters for which the optimal choices must be empirically determined by the user (Gross et al. 2016; Krueger et al. 2016). Unfortunately, there is no guideline provided for NTA about the experimental conditions and analytical methods involved in the study of NPs’ environmental behavior.

The objective of this study is to explore the actual aggregation process of NPs rather than classical plot of hydrodynamic diameter versus time, which has not been reported in the previous literatures. Firstly, according to representative research methods (Huangfu et al. 2013; Quik et al. 2014; Shih et al. 2012; Thio et al. 2011; Xu et al. 2016), CeO₂ NPs are chosen as model ENPs to examine the normal homo-aggregation kinetics by DLS and the result, which is consistent with the previous literatures, providing scientific basis to further evaluate the aggregation process by NTA. Then, the NTA method is used to investigate the drawbacks of DLS to study the aggregation process of NPs. A direct comparison between DLS and NTA is made to characterize the particle size distribution during the aggregation process. Furthermore, the relationship is established between the concentration of aggregates in the experiment and both two instruments’ detection limits. Toxicological studies have shown that NP toxicity depends on size, shape, surface charge, and their chemical composition (Behra et al. 2013; Hoecke et al. 2011; Karlsson et al. 2008; Shaw and Handy 2011). Aggregation process can change NP physical morphology, resulting in different toxicity results. Consequently, a clear understanding of the aggregation process is crucial to fully elucidate the fate and transport mechanisms of NPs in the environment and will enhance our understanding of the toxicity of NPs in an aquatic environment. The findings are also expected to provide guidelines for the experimental conditions and analytical methods in the study of NPs’ aggregation kinetics.

Materials and methods

Nanoparticles and suspensions

CeO₂ NPs (25 nm) were purchased from Sigma-Aldrich (Shanghai, China). The stock solutions were prepared by dissolving 50 mg of the CeO₂ NP powder in a 500-mL beaker with 500 mL of Milli-Q water

(18.2 MΩ cm⁻¹, Millipore, USA). The pH of the CeO₂ NP stock suspensions was 5.8, as measured by a pH meter (MPT-2, Malvern Instruments Ltd., UK). The stock suspensions were shaken by hand for 30 s and then sonicated in a homogenizer (1200 W, 25 kHz, Biosafe1200-98, China) for 30 min at 1200 W and 25 kHz (Qi et al. 2013). KCl and CaCl₂ were purchased from Aladdin Reagents (Shanghai, China), and the stock solutions were filtered through 0.22-μm filters before use. All the solutions were stored at 4 °C in the dark prior to use (Li and Chen 2012). The CeO₂ NP stock dispersions were characterized using several techniques.

NTA method

In order to better judge and interpret the NTA results, the influence of the parameter settings on the obtained results was investigated through the optimal particle concentrations and size distributions before the experiments. All NTA measurements were performed on the NanoSight 300 system and analyzed by NTA 3.2 software (Malvern Instruments Ltd., UK). The samples used for the NTA measurements were obtained by diluting each stock suspension (100 mg/L) to suitable multiples. When the top plate of the flow cell was cleaned, 1 mL of sample was placed in a syringe and slowly introduced into the test chamber. Then, the NTA software started to run, and the camera settings, including the screen gain (SG) and camera level (CL), were adjusted so that all particles were visible. The focus was optimized to ensure clear and sharp images of the particles. Finally, standard measurements were performed, and the detection threshold (DT) was adjusted as needed (Gross et al. 2016). Standard software settings for stock solution analysis in this study were: camera level 7, screen gain 10, detection threshold 15, and blur: auto. All measurements were performed in triplicate at 25 ± 0.3 °C, and the error lines represent the standard deviation of the three measurements. To provide more accurate size distributions and to avoid misinterpretation of the data, NanoSight software normally offered the finite track length adjustment (FTLA) data by modifying the raw data. The adjustment includes optimizing the particle size distributions and averaging the particles tracked during the total time of recording (Gallego-Urrea et al. 2011). However, raw data can contribute to the detection of small amounts of large particles such as aggregation kinetics. Therefore, in this study, two different modes for measuring of data were performed in the aggregation kinetics experiments.

Understanding aggregation kinetics

In order to obtain convincing data, the aggregation kinetics was assumed to be the same as those described by Li and Chen (2012). The concentrations of the electrolytes were within the following range: KCl, 0–100 mM; CaCl₂, 0–50 mM. The particle analyzer (ZetaSizer Nano ZSP, Malvern Instruments Ltd., UK) system was used to measure the increase of CeO₂ particle average hydrodynamic diameter with time. For the measurements, 0.5 mL of KCl (or CaCl₂) and 0.5 mL of the CeO₂ NP suspension were placed in a polystyrene measurement cell. The cell was then shaken slightly and immediately placed in the Zetasizer. The DLS equipment read the NP size every 21 s and each measurement consisted of three replicates, therefore, more than 60 data points were recorded in 1 h (Li and Chen 2012).

For the live monitoring of the CeO₂ NPs aggregation, 100 mM KCl and 10 mM CaCl₂ solutions were chosen as representative salt concentrations. The mixture solution, which was the same as that used in the DLS measurements, was introduced into the NanoSight NS300 sample chamber by a syringe. Four 60 s videos were recorded for each sample after 15, 30, 45, and 60 min of aggregation kinetics (Zheng et al. 2013).

Experimental mass concentration impact

For measurements of the aggregation rate, the mass concentration range of the CeO₂ NPs was 0.1–100 mg/L. In order to eliminate the effect of salt concentrations on the aggregation rate, a premeasured amount of KCl was mixed with 1 mL of the CeO₂ NP suspension in a cuvette to ensure that the aggregation rate constants were measured under favorable aggregation conditions (Chen et al. 2006). The details of the experiment were the same as those described in [Understanding aggregation kinetics](#).

Results and discussion

Characterization of CeO₂ NPs

The properties of the CeO₂ NPs in the stock suspension (100 mg/L) are presented in Fig. S1. The powder XRD analysis showed that the CeO₂ NPs exhibited a typical fluorite-like cubic structure (Fig. S1A). The scanning electron microscope (SEM) images (Fig. S1B) showed

that CeO₂ NPs were nearly spherical and relatively uniform, indicating that the NPs were evenly dispersed (Lv et al. 2016). The *z*-average diameter and zeta potential measured by DLS were 122 ± 12 nm and 36 ± 4 mV, respectively. The size distribution was measured using DLS and NTA, and the data in Fig. S1C showed that the primary particle size varied in the range of 50 to 250 nm for DLS measurements and 50 to 150 nm for NTA measurements. The polydispersity indices (PDI) reported from the DLS analysis for stock suspension is 0.13 ± 0.02, indicating that CeO₂ NPs are highly monodispersed (Busch et al. 2015; Li and Chen 2012). However, it should be noted that different peak areas were observed during the measurement of size distribution of the stock solutions. The peak area decreased in the following order: DLS > NTA raw data > NTA FTLA data. Fig. S1C also showed that the raw data yielded a particle concentration of 5.56 × 10⁷ ± 2.37 × 10⁶ particles/mL, which is much higher than that obtained from the FTLA data (1.89 × 10⁷ ± 1.56 × 10⁵ particles/mL). Moreover, the narrower peak distribution and smoother line in the FTLA data revealed that the sample was fairly monodisperse, but such features might probably be less accurate representations of the data (van der Pol et al. 2014).

DLS is known to have a major drawback in technique principles, which makes this technique very sensitive to the presence of large particles. The size distribution of stock suspension in this study towards larger sizes is probably caused by dust particles or small amounts of aggregates. Nur et al. (2015) reported that it was difficult to obtain a suspension of primary NPs even after sonication. Unlike DLS, NTA tracks individual particles and yields their size distribution along with a real-time view of the nanoparticles being measured, independent of the particle density (Hole et al. 2013). More specifically, the NTA 3.2 software provides raw and FTLA data for users to better understand the polydispersity of their samples. To obtain more “accurate” results (FTLA data), the software automatically corrects the raw data several times to avoid misinterpretation (Gallego-Urrea et al. 2011). Nevertheless, the unknown modifications to the data probably eliminate large particles, which are considered to be experimental errors by the NTA software. From Fig. S1C, compared with the raw data, the FTLA data with lower concentration and narrower particle size distribution indicated that the software automatically optimizes “undesired” data. Van Der Pol et al. (2014) compared the results of raw data and FTLA data in measuring the particle size distribution and found that

FTLA was not suitable for the measurement of polydisperse samples. Therefore, the size distribution of the NPs from NTA requires careful interpretation.

Overall, despite of the drawbacks, DLS is the most user-friendly NP size characterization technique, which is the most frequently used in the study of aggregation kinetics (Hole et al. 2013; Huangfu et al. 2013; Lin et al. 2016b; Miao et al. 2016). The DLS method in this study is used to determine *z*-average hydrodynamic diameter and the size distribution of CeO₂ NPs in different salt solutions. A direct comparison with NTA FTLA data is made to reveal the pitfalls of DLS in the field of characterization of aggregation kinetics. The raw data is also used in this analysis because the raw size distributions are more precise reflections of the changes in aggregation, and fitting the results with a software model would distort the actual data (Lawler et al. 2015).

NTA method

Experimental parameters setting

As mentioned above, the NTA software involves several settings that affect the accuracy of the measurement results. In order to gain a comprehensive understanding on NTA instruments and software, the effect of each parameter was carefully analyzed, as shown in Fig. 1. Standard analysis yielded a particle size of 122 ± 0.9 nm and a particle concentration of $1.02 \times 10^9 \pm 5.39 \times 10^7$ particles/mL for the stock suspension, indicating a relatively monodisperse sample. However, higher CL, higher SG, or lower DT could all increase the particle concentration, leading to the overestimation of measured particle concentration. Meanwhile, the size of CeO₂ NPs sharply decreased with increased particle concentration.

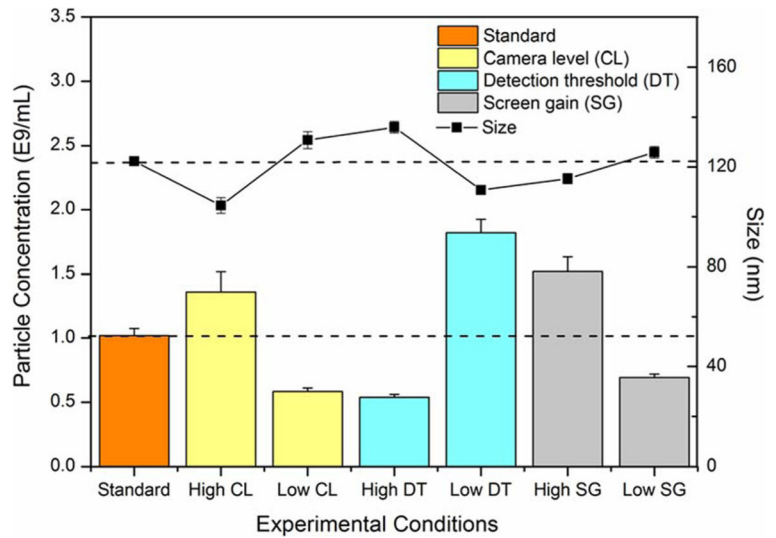
The CL and SG are parameters for the NTA camera to give a more linear increase in brightness across the imaging range. This means that the same sample would be characterized by different particles at different camera levels. Following the instructions in the NanoSight 300 NTA Software Guide (Malvern Instruments Ltd., UK), the CL and SG will be increased until all the particles in the sample could be seen clearly, but no more than 20% are saturated. A higher CL and SG could also yield colored pixels so that some primary particles are tracked repeatedly, and the measured concentration would be significantly overestimated (Gross et al. 2016). Furthermore, owing to the use of the stock

suspension for the measurements, the primary particles that were repeatedly tracked decreased the mean size (Fig. 1). In contrast, a lower CL and SG could leave the camera with insufficient brightness to track the small particles in the NTA capture screen, which would result in lower particle concentration and higher particle size. Since the DT determines the minimum brightness of pixels to be considered for tracking, the lower the setting, the more particle centers would be found. However, if DT is too low, the “noise” can be tracked, which results in an overestimation of the particle concentration and an underestimation of the particle size. On the other hand, if the DT setting is too high, particles will be excluded and an inaccurate result will be obtained. These findings are in accordance with those of Gross et al. (2016) who demonstrated that the choice of parameters (CL, DT, or SG) can significantly affect NTA results (Gross et al. 2016). This section also clearly showed a direct relationship between the particle size and the concentration measured by NTA. Incorrect parameter settings mainly affect the measurement of small primary particles and the overestimated concentration reduced the average particle size of the solution. This phenomenon is probably more evident in the measurement of polydisperse solutions by NTA.

The effect of measurement time

The effect of measurement time on the NTA results was investigated to explore the potential use of NTA in analyzing the NP aggregation process. Figure 2 shows that the particle concentration decreased significantly with the measuring time. At $t_{0\text{min}}$, the highest peak was detected, which indicates that the particle concentration was around 3.3×10^7 particles/mL. The peak shifted to the right and decreased over time. At $t_{60\text{min}}$, the peak was almost invisible and the size distribution was very wide. At $t_{\text{reflowing}}$ when the solution in the test chamber was reflowing using the syringe, the peak was detectable again. This finding is inconsistent with the observations reported by Filipe et al. (2010), who reported that NTA was very suitable for analyzing protein aggregates and provided information on their aggregation. A plausible explanation for this is that since the measurement temperature used in the experiments by Felipe et al. was 50 °C, the particles moved faster than usual and a sufficient number of these particles could be tracked within the time frame of the experiments. Since the experiment in the present study was conducted at

Fig. 1 The particle concentration and size of CeO₂ NP stock solution (100 mg/L) in various experimental parameters measured by NTA. (SG, screen gain; CL, camera level DT, detection threshold)



room temperature, some particles settled to the bottom or moved out of focus in the detection area, making particle tracking more difficult for the NTA software. After reflowing of the solution using the syringe, the particles at the bottom were re-suspended in the test chamber and more particles could be tracked in the field of view. Consequently, the results indicated that NTA may not be suitable for measuring the aggregation kinetics. Nevertheless, NTA is still a powerful characterization technique used in conjunction with DLS for

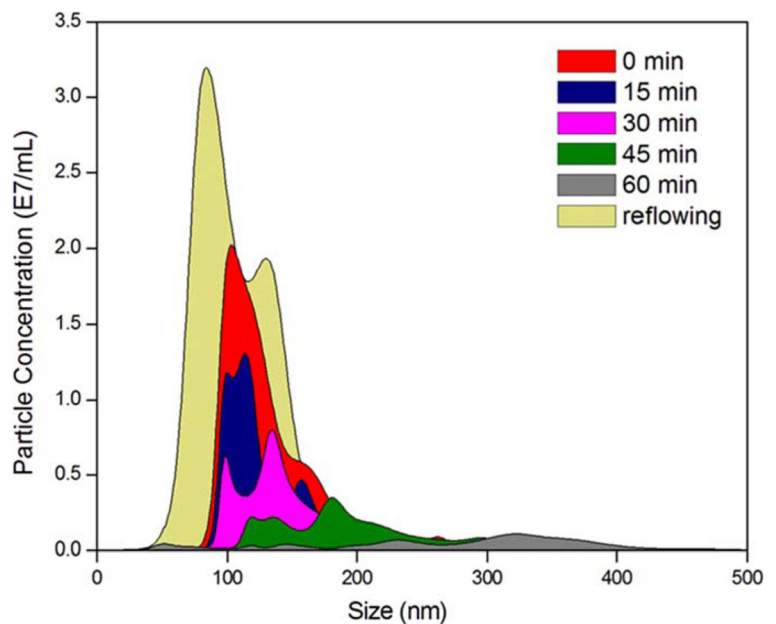
analyzing the behavior of NPs in an aquatic environment, which will be discussed in the following section.

Understanding of aggregation kinetics

Use DLS alone

Fig S2 shows the representative aggregation kinetics curves of CeO₂ NPs in the KCl and CaCl₂ solutions which are obtained using DLS measurements. As

Fig. 2 Particle concentrations of CeO₂ NP stock suspension at different measuring times measured by NTA



expected, in the low ionic strength (IS) ranges of KCl (2.5 mM) and CaCl₂ (0.5 and 2 mM), the aggregation curves were almost horizontal lines, indicating that no aggregation was observed. When the concentrations of KCl and CaCl₂ were higher than 5 and 4 mM, respectively, the rate of aggregation increased with increasing cation concentration. Finally, the aggregation rate reached the maximum when the KCl concentration was above 20 mM and the CaCl₂ concentration was above 6 mM. The similar fastest aggregation was observed for CeO₂ in 50 mM KCl and 8 mM CaCl₂, through charge neutralization by completely compressing the electrical double layer (Chekli et al. 2013, 2015; Chen et al. 2010).

As usual, the DLVO theory is always used to analyze the aggregation behavior of nanoparticles (Bian et al. 2011; Chen and Elimelech 2006; Chen et al. 2006; Shih et al. 2012). This theory assumes that the interaction of dispersed particles involves a balance between the van der Waals attraction and the electrical double-layer repulsion. In the presence of a relatively low concentration of KCl or CaCl₂, the electrical double-layer repulsive energy was dominant and no aggregation was observed. An increase in IS would lead to a significant decrease in the repulsive forces among the particles, resulting in rapid aggregation rates. When IS in the solution reaches the critical coagulation concentration (CCC), which usually refers to the minimum electrolyte concentration that could completely eliminate the surface charge of particles, the aggregation rate reaches maximum. The CCC values in this study were about 50 and 6 mM for KCl and CaCl₂, respectively, which are similar to the values reported by Li and Chen (2012). Overall, these findings can provide information on the particle aggregation characteristics. However, it is unclear how much remains unknown regarding nanoparticles in the aggregation process.

Combined use of DLS and NTA

In order to investigate the behavior of nanoparticles in the aggregation kinetics, the size distributions of CeO₂ NPs in different salt solutions were measured using both DLS and NTA, and the results are shown in Fig. 3. After the beginning of aggregation for 15 min, the particle size measured by DLS was between 400 and 1000 nm, with a peak at 600 nm in both salt solutions, while the particle size was in the range of 50 to 400 nm according to the NTA FTLA data. After about 30 min, the size distribution

obtained by DLS and NTA were almost unchanged and the peak for the mixtures shifted slightly towards the larger particle size for the DLS data. Similar results were obtained for 60 min after the beginning of the experiment. The similar trends in particle size distributions in both KCl and CaCl₂ solutions reflect the samples' actual content. The current data, which show that the aggregation process was more complicated than previously thought, give a more complete understanding on the aggregation mechanism of NPs. The results in Fig. 3 indicated that not all particles in water aggregated together by DLVO or non-DLVO forces, and many small CeO₂ NPs remained unattached in the solution. Furthermore, the size of the aggregated particles was far smaller than the value obtained in the aggregation kinetics experiment, although the presence of cations could lead to charge neutralization by compressing the electrical double layer of NPs and promoted aggregation of the nanoparticles (Chekli et al. 2015; Shih et al. 2012; Thio et al. 2011). This phenomenon that not all the particles aggregated together can be explained by collision efficiency. The collision efficiency which expresses the ability when two particles collide and form an aggregate, plays a very important role in the aggregation kinetics between particles, which depends on the electrolyte concentration, pH, particle concentration, point of zero charge, and temperature (Anne-Archard et al. 2013; Arvidsson et al. 2011; Cunha and Couto 2011; Hu et al. 2003). Cunha and Couto reported that hydrodynamic interactions have a strong impact on the collision efficiency during the aggregation process (Cunha and Couto 2011). Arvidsson et al. (2011) found that the collision efficiency is very sensitive to the concentration of natural organic matter (NOM). Table S2 shows that the polydispersity index (PDI) in the process of aggregation under conditions of 100 mM KCl and 10 mM CaCl₂ were in the range of 0.33–0.64 and 0.31–0.62, respectively, indicating that the NP solution in the aggregation process was a highly polydispersed system (Busch et al. 2015; Gillespie et al. 2011). That also indicated that the collision efficiency significantly influences ($p < 0.05$) the aggregation process even without hydrodynamic interactions with NOM. In fact, random collisions invariably occur among the particles that undergo Brownian motion in the solution, but only the effective collisions can lead to the aggregation of nanoparticles.

The results of this study show very important environmental significance. The size data measured by DLS do not really reflect the particle size distribution in the samples, which has an important effect on its potential toxicity

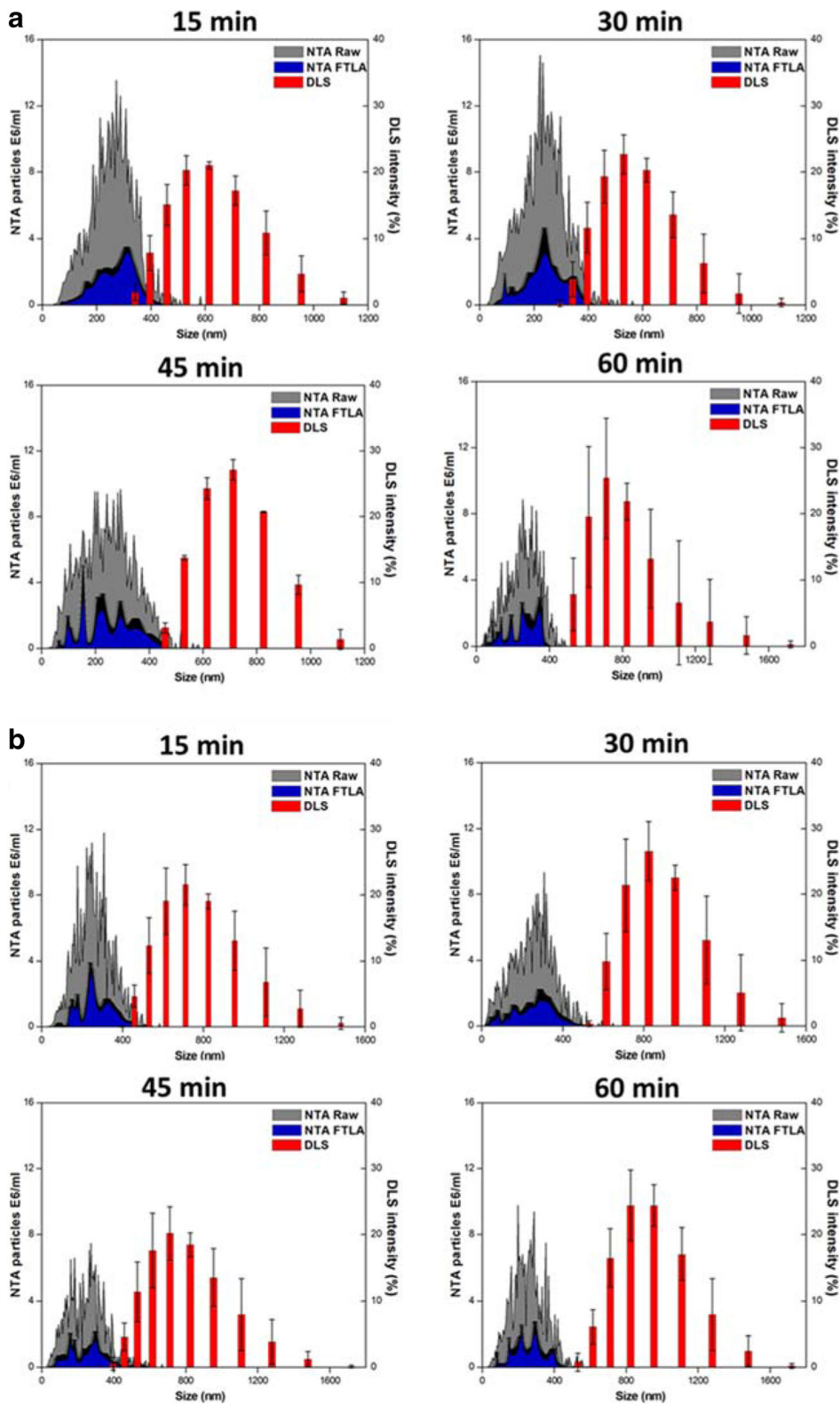


Fig. 3 Size distribution in the process of aggregation kinetics in the (a) KCl solution (100 mM) and (b) CaCl₂ solution (10 mM) measured with DLS and NTA (CeO₂ concentration: 10 mg/L)

study in aquatic environment. Previous ecotoxicity tests had showed that the NP toxicity exhibited a small size effect that nominally smaller NPs are more toxic than larger NPs (Hoecke et al. 2011; Joo and Zhao 2016). For instance, Zhang et al. (2012) reported that the toxicity of NPs in various solutions should increase in the order of $\text{MgCl}_2 < \text{CaCl}_2 < \text{KCl}$ since the sizes of NP aggregates in the CaCl_2 and MgCl_2 solutions were much larger than those in the KCl solution. Hoecke et al. (2009) chose three different sizes of CeO_2 NPs for aquatic toxicity tests and results showed that chronic toxicity was found to increase with decreasing nominal particle diameter. According to our study, some of the small aggregates were neglected by DLS in various solutions. Unfortunately, they may play a decisive role in toxicological experiments. Therefore, the hypothesis that the decreased toxicity co-occurs with increasing aggregation of NPs may need to be reconsidered.

However, although there are some studies that reported the complexity of the aggregation process in environmental samples, the majority of literatures presented the standard aggregation process, in which the aggregation rate or attachment efficiency could always be obtained (Huangfu et al. 2013; Liu et al. 2013; Shih et al. 2012; Thio et al. 2011). In contrast, many evidences from our present study indicated that even in a simple system with only salt and NPs, the classic aggregation kinetics theory cannot sufficiently or precisely describe particle aggregation, and there remains a discrepancy between the size distributions obtained by theoretical analysis and experimental observations. Therefore, more rigorous experiments should be developed to describe the aggregation process rather than only the averaged hydrodynamic diameter or mean size (Huangfu et al. 2013; Shih et al. 2012).

Figure 4 presents the size distributions obtained from DLS and NTA measurements after particle aggregation in various electrolyte solutions. In the 0.5 and 2 mM CaCl_2 solutions, the size distributions obtained by DLS and NTA measurements were consistent with the fact that the nanoparticles did not aggregate in the solutions. This conclusion is not only consistent with the experimental observation of the aggregation kinetics (Fig. S2), but also indicates that the NTA equipment parameters are set correctly. The size distributions obtained from the DLS measurements increased with increasing cation concentration and ranged from 400 to 2000 nm in 100 mM KCl and 600 to 2000 nm in 10 mM CaCl_2 , suggesting that the broad distributions and high error bars were mostly caused by large aggregates.

Remarkably, the difficulty for DLS to distinguish small particles in polydisperse solutions became apparent, as it could not detect particles smaller than 400 nm (Fig. 4). On the other hand, surprisingly, the NTA technique yielded a relatively narrow size distribution and did not detect particles larger than 800 nm for all polydisperse samples. However, the detection limit of NTA is in the range of 30–1000 nm, suggesting that aggregates smaller than 1000 nm should be individually tracked and calculated (Griffiths et al. 2011). A possible explanation for the inconsistency is that the large (> 400 nm) aggregates were broken by a slight shear force during injection (by syringe) into the NTA measurement cell (Filipe et al. 2010). In addition, as previously mentioned in Fig. 2, it is increasingly clear that shear can affect the aggregation state during NTA measurements.

The NTA software generated raw and FTLA data for the characterization of NPs in a suspension. As can be seen in the figures, the aggregate size distribution was consistent in the two sets of data, with a narrow range between 50 to 400 nm. However, additional information about the size distribution can still be obtained from the raw data. The size distributions from 50 to 500 nm with a rougher line and a sharper peak were observed in the raw data in all figures, which indicated that the solution might be more complicated than the result presented by the FTLA data. Interestingly, some large (> 400 nm) aggregates were visible through the raw data, but they disappeared from the FTLA data. It is known that the NTA software makes several corrections to the raw data in order to provide a more “precise” size distribution and to avoid misinterpretation of the obtained data (Gallego-Urrea et al. 2011). The details of the corrections to the raw data are not available to the user, which makes it difficult to evaluate and assess the NTA results. Therefore, a possible explanation is that the NTA software in this study smoothed the particle size distributions and removed the large particles detected by the raw data as they were considered impurities, resulting in the smoother, but less accurate representation of the data (van der Pol et al. 2014).

Experimental mass concentration impact

The impact of mass concentration on NTA measure

It is well known that the disadvantage of NTA is that it requires a higher sample concentration than DLS, which limits further development and wider application of the

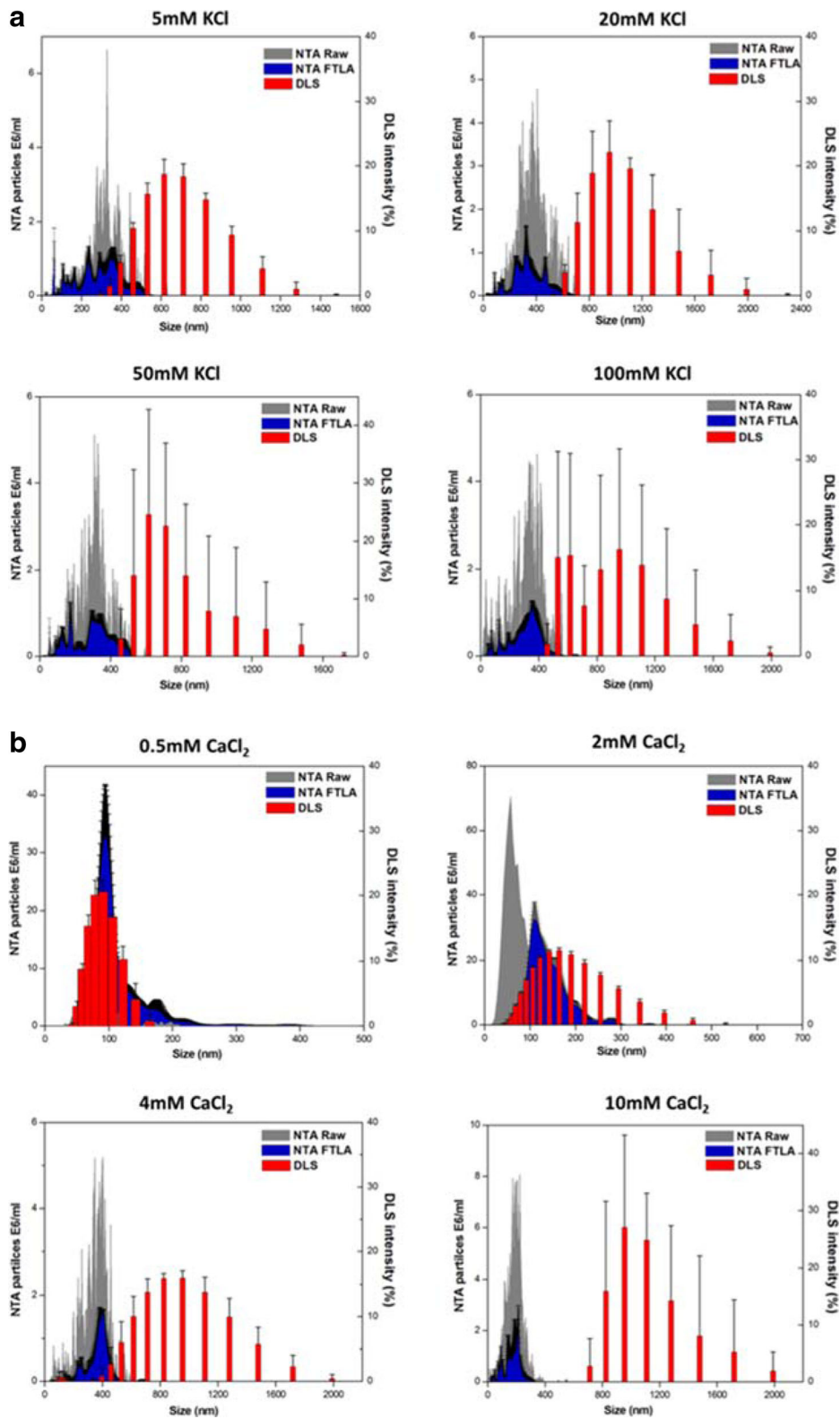
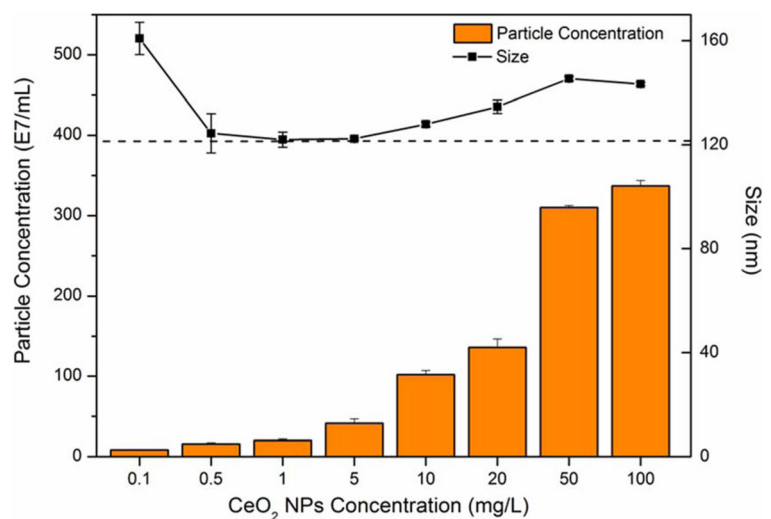


Fig. 4 Size distribution from NTA and DLS measurements of CeO₂ NPs (10 mg/L) after aggregation kinetics in various electrolyte solutions: **(a)** KCl (5, 20, 50, 100 mg/L) and **(b)** CaCl₂ (0.5, 2, 4, 10 mg/L)

technique (Vasco et al. 2010). Hence, the objectives of this section were to investigate the appropriate mass concentration of CeO₂ NPs for potential use of NTA in measuring the size and particle concentration in aggregation experiments. Figure 5 shows the detected particle concentration and size of CeO₂ NPs in stock solutions of different mass concentrations. The specific values can be seen in Table.S3.

As expected, the particle concentration increased with increasing mass concentration. However, the size of CeO₂ NPs fluctuated according to the mass concentration, and the CeO₂ particle size deviated from the standard value (122 nm) at a mass concentration below 0.5 mg/L or above 10 mg/L. Of particular concern are the large deviations in the measured particle size in the stock solution. Although the particle concentration of the stock solution did not exceed the detection range of the instrument (10^7 – 10^9 total particles/mL), the optimal result could not be obtained if the mass concentration was too high or too low (Filipe et al. 2010). In fact, particles in the liquid sample that passed through the beam path moved rapidly under Brownian motion, allowing information on the particle properties to be obtained. A much higher sample concentration could have prevented accurate particle tracking, while a much lower sample concentration would not have produced a statistically significant result (Hole et al. 2013). It is noted that the experimental trend was not significant since the sample used was the stock suspension, which was the monodisperse solution. Once the sample became complex and unstable, the effect on the results became more significant.

Fig. 5 Particle concentration and size of stock solution in various CeO₂ NP mass concentrations measured by NTA

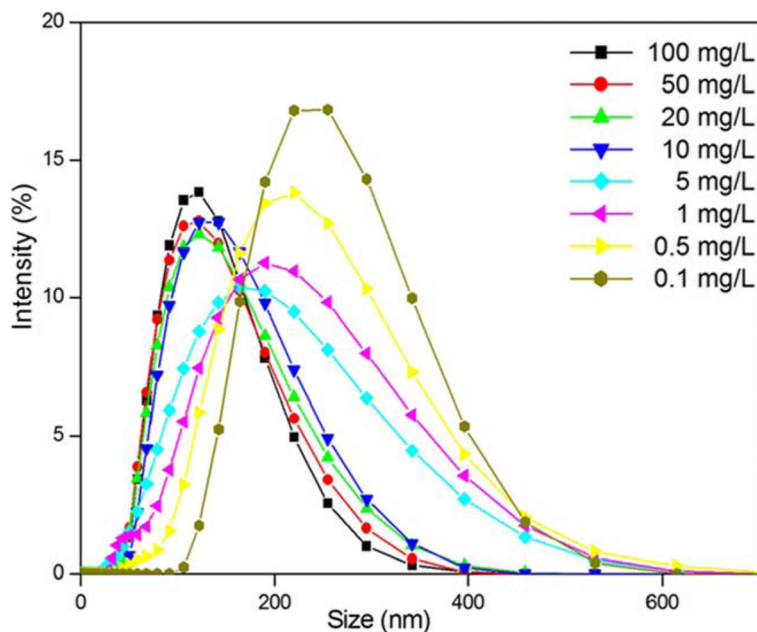


The most important finding in Fig. 5 was that NTA can measure samples with concentration ranging from 0.1 to 100 mg/L, which would satisfy the requirements of most studies on the life cycle and behavior of NPs (Keller et al. 2010; Chekli et al. 2015; Hoecke et al. 2011; Quik et al. 2014). Prior to our study, NTA was generally considered unable to reflect the actual behavior of NPs in an aquatic environment because of the narrow range of measurements, which means high-concentration samples always need to be diluted before each measurement (Dragovic et al. 2011a; Filipe et al. 2010; Gross et al. 2016). In the aggregation process, the sufficient collision that produces larger aggregates is directly proportional to the number concentrations (Lv et al. 2016). When a stock solution is diluted, the collision efficiency is different because of the lower particle concentration, leading to a different aggregation rate. However, it is revealed by our study that accurate measurement results can be obtained by adjusting the parameters of the NTA equipment without further dilution.

The relationship between the experimental mass concentration and detection limits in DLS measurement

In order to explore the relationship between the experimental concentration and the experimental detection limits, the aggregation kinetics was investigated using different CeO₂ NP mass concentrations and time-resolved dynamic light scattering. Figure 6 shows the particle size distribution of CeO₂ NPs in stock solutions of different mass concentrations. When the stock concentration was greater than 5 mg/L, the peak value did

Fig. 6 Particle size distribution of CeO₂ NPs in stock solutions of different mass concentrations



not change with the measured concentration, suggesting that the measurements were accurate. The peak for the stock solution shifted towards larger particle sizes as the experimental concentration decreased. The size given by DLS was 304.4 ± 34.1 nm at a stock concentration of 0.1 mg/L (Table S4), which is much larger than normal. Considering that the samples were monodisperse stock suspensions, such a big error cannot be ignored. Traditional light-scattering techniques (such as DLS) measure the fluctuation in scattering intensity of NPs and then use this information to calculate the size of the particles through the Stokes–Einstein equation (Zetasizer Nano User Manual, Malvern Instruments, UK). The scattering intensity can thus be directly related to the solution molecular mass of the sample (Philo 2009). Therefore, the large error was obtained probably because the light-scattering intensity was too low for accurate calculation when the NP concentration was too low.

The aggregation kinetics with different CeO₂ NP mass concentrations in the presence of 100 mM KCl is shown in Fig. S3. At high CeO₂ NP concentrations (i.e., 10, 20, and 50 mg/L), increasing in nanoparticle concentration led to a corresponding increase in the aggregation rate. These results are consistent with the classic DLVO theory. At electrolyte concentrations above the CCC, the aggregation rate is completely dependent on the particle number concentration, the

diffusion of the particles, and the collision efficiency (Huangfu et al. 2013; Liu et al. 2012, 2013; Shih et al. 2012). This result also indicates the flaw of aggregation kinetics, where the selection of initial particle mass concentration directly determines the results of the aggregation experiment. Interestingly, when the mass concentration of CeO₂ NPs was lower than 1 mg/L, the size of CeO₂ NP was stable even when the KCl concentration was higher than the CCC. Generally, aggregation occurs invariably between particles in samples when the electrolyte concentration is above the CCC. This happens because when the sample concentration is extremely low and the particle concentration decreases during the aggregation process with time, the scattering intensity detected by DLS is too low for accurate calculations. This result indicates that there exists limited detection concentration in the measurement of aggregation kinetics by DLS. For instance, Chekli et al. (2015) reported that the final concentration of citrate-Ag NPs in aggregation study of natural waters was 1 mg/L. According to our results, this concentration may not reach the sufficiently strong signal on the DLS. Additionally, Praetorius et al. (2014) investigated the heteroaggregation kinetics between TiO₂ NPs and Suwannee River humic acid and the measurements were performed at a TiO₂ concentration of 0.8 mg/L. However, due to the detection limit of

DLS, most of the aggregation data obtained by DLS in this study may be caused by humic acid homo-aggregation.

Conclusions

The results of size distribution from NTA and DLS measurements demonstrated that the aggregation process is more complicated than previously thought, as not all particles in the water aggregated together and there still exist lots of small CeO₂ particles (< 400 nm). Furthermore, the size of the aggregated particles is far smaller than the value obtained by aggregation kinetics experiment. Interestingly, according to the results of this paper, samples with concentrations ranging from 0.1 to 100 mg/L can be measured by NTA, which is wider than the expected detection limit. Additionally, the accurate measurement results may be obtained by adjusting the parameters of the NTA without further dilution. In contrast, DLS cannot offer accurate result about particle size when the mass concentration of CeO₂ NPs is lower than 1 mg/L.

In conclusion, due to the intrinsic technique principles, the classical aggregation kinetics results obtained from DLS may not reflect the accurate behavior of NPs in an aquatic environment, let alone the heteroaggregation of NPs in complex water phase. Thus, strict and the wide size distribution among the samples should be a serious concern. Furthermore, no single analytical technique can offer a comprehensive understanding on the aggregation process of NPs. NTA and DLS exhibit individual and special advantages and only the combined application of these two techniques can truly characterize the nanoparticles in the aggregation process. It is believed that these findings will provide a guide for the experimental conditions and analytical methods in the study of aggregation kinetics.

Funding information We are grateful for the grants for Project supported by the National Science Funds for Creative Research Groups of China (No.51421006), the National Natural Science Funds for Excellent Young Scholar (No.51722902), the Key Program of National Natural Science Foundation of China (No. 91647206), the Outstanding Youth Fund of Natural Science Foundation of Jiangsu, China (BK20160038), and PAPD.

Compliance with ethical standards

Conflict of interest The authors declare that they have no conflict of interest.

References

- Anne-Archard D, D'Olce M, Tourbin M, Frances C (2013) Aggregation of silica nanoparticles in concentrated suspensions under turbulent, shear and extensional flows. *Chem Eng Sci* 95:184–193
- Arvidsson R, Molander S, Sandén BA, Hassellöv M (2011) Challenges in exposure modeling of nanoparticles in aquatic environments. *Hum Ecol Risk Assess Int J* 17:245–262
- Baalousha M, Nur Y, Römer I, Tejamaya M, Lead JR (2013) Effect of monovalent and divalent cations, anions and fulvic acid on aggregation of citrate-coated silver nanoparticles. *Sci Total Environ* 454–455:119–131
- Behra R, Sigg L, Clift MJ, Herzog F, Minghetti M, Johnston B, Petrifink A, Rothenrutishauser B (2013) Bioavailability of silver nanoparticles and ions: from a chemical and biochemical perspective. *J R Soc Interface* 10:20130396
- Bian SW, Mudunkotuwa IA, Rupasinghe T, Grassian VH (2011) Aggregation and dissolution of 4 nm ZnO nanoparticles in aqueous environments: influence of pH, ionic strength, size, and adsorption of humic acid. *Langmuir* 27:6059–6068
- Busch VM, Loosli F, Santagapita PR, Buera MP, Stoll S (2015) Formation of complexes between hematite nanoparticles and a non-conventional galactomannan gum. Toward a better understanding on interaction processes. *Sci Total Environ* 532:556–563
- Cekli L, Phuntsho S, Roy M, Lombi E, Donner E, Shon HK (2013) Assessing the aggregation behaviour of iron oxide nanoparticles under relevant environmental conditions using a multi-method approach. *Water Res* 47:4585–4599
- Cekli L, Zhao YX, Tijing LD, Phuntsho S, Donner E, Lombi E, Gao BY, Shon HK (2015) Aggregation behaviour of engineered nanoparticles in natural waters: characterising aggregate structure using on-line laser light scattering. *J Hazard Mater* 284:190–200
- Chen KL, Elimelech M (2006) Aggregation and deposition kinetics of fullerene (C₆₀) nanoparticles. *Langmuir* 22:10994–11001
- Chen KL, Mylon SE, Elimelech M (2006) Aggregation kinetics of alginate-coated hematite nanoparticles in monovalent and divalent electrolytes. *Environ Sci Technol* 40:1516–1523
- Chen KL, Smith BA, Ball WP, Fairbrother DH (2010) Assessing the colloidal properties of engineered nanoparticles in water: case studies from fullerene C₆₀ nanoparticles and carbon nanotubes. *Environ Chem* 7:10–27
- Cunha FR, Couto HLG (2011) On the influence of the hydrodynamic interactions on the aggregation rate of magnetic spheres in a dilute suspension. *J Magn Magn Mater* 323: 77–82
- Dragovic RA, Gardiner C, Brooks AS, Tannetta DS, Ferguson DJ, Hole P, Carr B, Redman CW, Harris AL, Dobson PJ (2011a) Sizing and phenotyping of cellular vesicles using nanoparticle tracking analysis. *Nanomedicine* 7:780–788
- Dragovic RA, Gardiner C, Brooks AS, Tannetta DS, Ferguson DJ, Hole P, Carr B, Redman CW, Harris AL, Dobson PJ, Harrison P, Sargent IL (2011b) Sizing and phenotyping of cellular vesicles using nanoparticle tracking analysis. *Nanomedicine* 7:780–788

- Elizabeth MDO, Adriana DSFA, De Castro JA (2014) Application of nanoparticle tracking analysis (NTA) in aqueous solutions of TiO₂. *Mater Sci Forum* 802:624–629
- Filipe V, Hawe A, Jiskoot W (2010) Critical evaluation of nanoparticle tracking analysis (NTA) by NanoSight for the measurement of nanoparticles and protein aggregates. *Pharm Res* 27:796–810
- Gallego-Urrea JA, Tuoriniemi J, Hassellöv M (2011) Applications of particle-tracking analysis to the determination of size distributions and concentrations of nanoparticles in environmental, biological and food samples. *Trends Anal Chem* 30: 473–483
- Gallego-Urrea JA, Hammes J, Cornelis G, Hassellöv M (2016) Coagulation and sedimentation of gold nanoparticles and illite in model natural waters: influence of initial particle concentration. *Nanoimpact* 46:112–128
- Gillespie C, Halling P, Edwards D (2011) Monitoring of particle growth at a low concentration of a poorly water soluble drug using the NanoSight LM20. *Colloids Surf A Physicochem Eng Asp* 384:233–239
- Griffiths D, Bernt W, Hole P, Smith J, Malloy A, Carr B (2011) Zeta potential measurement of nanoparticles by nanoparticles tracking analysis. *NSTI-nanotech* 1
- Gross J, Sayle S, Karow AR, Bakowsky U, Garidel P (2016) Nanoparticle tracking analysis of particle size and concentration detection in suspensions of polymer and protein samples: influence of experimental and data evaluation parameters. *Eur J Pharm Biopharm* 104:30–41
- Hoecke KV, Quik JTK, Mankiewiczbozbek J, Schamphelaere KACD, Elsaesser A, Meeren PVD, Barnes C, Mckerr G, Howard CV, Meent DVD (2009) Fate and effects of CeO₂ nanoparticles in aquatic ecotoxicity tests. *Environ Sci Technol* 43:4537–4546
- Hoecke KV, Schamphelaere KACD, Meeren PVD, Smaghe G, Janssen CR (2011) Aggregation and ecotoxicity of CeO₂ nanoparticles in synthetic and natural waters with variable pH, organic matter concentration and ionic strength. *Environ Pollut* 159:970–976
- Hole P, Silence K, Hannell C, Maguire CM, Roesslein M, Suarez G, Capracotta S, Magdolenova Z, Horev-Azaria L, Dybowska A (2013) Interlaboratory comparison of size measurements on nanoparticles using nanoparticle tracking analysis (NTA). *J Nanopart Res* 15:1–12
- Hou J, You G, Xu Y, Wang C, Wang P, Miao L, Ao Y, Li Y, Lv B (2015) Effects of CeO₂ nanoparticles on biological nitrogen removal in a sequencing batch biofilm reactor and mechanism of toxicity. *Bioresour Technol* 191:73–78
- Hu Y, Qiu G, Miller JD (2003) Hydrodynamic interactions between particles in aggregation and flotation. *Int J Miner Process* 65:157–170
- Huangfu X, Jiang J, Ma J, Liu Y, Yang J (2013) Aggregation kinetics of manganese dioxide colloids in aqueous solution: influence of humic substances and biomacromolecules. *Environ Sci Technol* 47:10285–10292
- Jiskoot W, Crommelin DJA (2005) *Methods for structural analysis of protein pharmaceuticals*. Springer Verlag GmbH
- Joo SH, Zhao D (2016) Environmental dynamics of metal oxide nanoparticles in heterogeneous systems: a review. *J Hazard Mater* 322:29–47
- Karlsson HL, Cronholm P, Gustafsson J, Möller L (2008) Copper oxide nanoparticles are highly toxic: a comparison between metal oxide nanoparticles and carbon nanotubes. *Chem Res Toxicol* 21:1726–1732
- Keller AA, Wang H, Zhou D, Lenihan HS, Cherr G, Cardinale BJ, Miller R, Ji Z (2010) Stability and aggregation of metal oxide nanoparticles in natural aqueous matrices. *Environ Sci Technol* 44:1962–1967
- Krueger AB, Carnell P, Carpenter JF (2016) Characterization of factors affecting nanoparticle tracking analysis results with synthetic and protein nanoparticles. *J Pharm Sci* 105:1434–1443
- Lawler DF, Youn S, Zhu T, Kim I, Lau BL (2015) Comprehensive understanding of nano-sized particle separation processes using nanoparticle tracking analysis. *Water Sci Technol* 72: 2318–2324
- Lee J, Bartelt-Hunt SL, Li Y, Morton M (2015) Effect of 17β-estradiol on stability and mobility of TiO₂ rutile nanoparticles. *Sci Total Environ* 511:195–202
- Li K, Chen Y (2012) Effect of natural organic matter on the aggregation kinetics of CeO₂ nanoparticles in KCl and CaCl₂ solutions: measurements and modeling. *J Hazard Mater* 209–210:264–270
- Li Q, Chen B, Xing B (2017) Aggregation kinetics and self-assembly mechanisms of graphene quantum dots in aqueous solutions: cooperative effects of pH and electrolytes. *Environ Sci Technol* 51:1364–1376
- Lin D, Drew SS, Walker SL, Huang Q, Cai P (2016a) Influence of extracellular polymeric substances on the aggregation kinetics of TiO₂ nanoparticles. *Water Res* 104:381–388
- Lin D, Story SD, Walker SL, Huang QY, Cai P (2016b) Influence of extracellular polymeric substances on the aggregation kinetics of TiO₂ nanoparticles. *Water Res* 104:381–388
- Liu J, Legros S, Ma G, Veinot JG, von der Kammer F, Hofmann T (2012) Influence of surface functionalization and particle size on the aggregation kinetics of engineered nanoparticles. *Chemosphere* 87:918–924
- Liu J, Legros S, von der Kammer F, Hofmann T (2013) Natural organic matter concentration and hydrochemistry influence aggregation kinetics of functionalized engineered nanoparticles. *Environ Sci Technol* 47:4113–4120
- Loosli F, Coustumer PL, Stoll S (2015) Effect of electrolyte valency, alginate concentration and pH on engineered TiO₂ nanoparticle stability in aqueous solution. *Sci Total Environ* 535:28–34
- Lungu A, Lungu M, Neculăe A, Giugiulan R (2015) Nanoparticle characterization using nanoparticle tracking. *Analysis*. 245–268
- Lv B, Wang C, Hou J, Wang P, Miao L, Li Y, Ao Y, Yang Y, You G, Xu Y (2016) Influence of shear forces on the aggregation and sedimentation behavior of cerium dioxide (CeO₂) nanoparticles under different hydrochemical conditions. *J Nanopart Res* 18:193
- Mehrabi K, Nowack B, Dasilva YAR, Mitrano DM (2017) Improvements in nanoparticle tracking analysis to measure particle aggregation and mass distribution: a case study on engineered nanomaterial stability in incineration landfill leachates. *Environ Sci Technol* 51:5611–5621
- Miao L, Wang C, Hou J, Wang P, Ao Y, Li Y, Lv B, Yang Y, You G, Xu Y (2016) Effect of alginate on the aggregation kinetics of copper oxide nanoparticles (CuO NPs): bridging interaction and hetero-aggregation induced by Ca(+2). *Environ Sci Pollut Res* 23:11611–11619

- Nur Y, Lead JR, Baalousha M (2015) Evaluation of charge and agglomeration behavior of TiO₂ nanoparticles in ecotoxicological media. *Sci Total Environ* 535:45–53
- Oriekhova O, Stoll S (2016) Effects of pH and fulvic acids concentration on the stability of fulvic acids – cerium (IV) oxide nanoparticle complexes. *Chemosphere* 144:131–137
- Philo JS (2009) A critical review of methods for size characterization of non-particulate protein aggregates. *Curr Pharm Biotechnol* 10
- Piccinno F, Gottschalk F, Seeger S, Nowack B (2012) Industrial production quantities and uses of ten engineered nanomaterials in Europe and the world. *J Nanopart Res* 14: 1–11
- Pol EVD, Coumans FAW, Sturk A, Nieuwland R, Leeuwen TGV (2014) Refractive index determination of nanoparticles in suspension using nanoparticle tracking analysis. *Nano Lett* 14:6195–6201
- Praetorius A, Labille J, Scheringer M, Thill A, Hungerbühler K, Bottero JY (2014) Heteroaggregation of titanium dioxide nanoparticles with model natural colloids under environmentally relevant conditions. *Environ Sci Technol* 48:10690–10698
- Qi J, Ye YY, Wu JJ, Wang HT, Li FT (2013) Dispersion and stability of titanium dioxide nanoparticles in aqueous suspension: effects of ultrasonication and concentration. *Water Sci Technol* 67:147–151
- Quik JT, Lynch I, Van HK, Miermans CJ, De Schampelaere KA, Janssen CR, Dawson KA, Stuart MA, Van DMD (2010) Effect of natural organic matter on cerium dioxide nanoparticles settling in model fresh water. *Chemosphere* 81:711–715
- Quik JTK, Velzeboer I, Wouterse M, Koelmans AA, Meent DVD (2014) Heteroaggregation and sedimentation rates for nanomaterials in natural waters. *Water Res* 48:269–279
- Romerofranco M, Godwin HA, Bilal M, Cohen Y (2017) Needs and challenges for assessing the environmental impacts of engineered nanomaterials (ENMs). *Beilstein J Nanotechnol* 8:989–1014
- Shaw BJ, Handy RD (2011) Physiological effects of nanoparticles on fish: a comparison of nanometals versus metal ions. *Environ Int* 37:1083–1097
- Shih YH, Zhuang CM, Peng YH, Lin CH, Tseng YM (2012) The effect of inorganic ions on the aggregation kinetics of lab-made TiO₂ nanoparticles in water. *Sci Total Environ* 435–436:446–452
- Sotirelis NP, Chrysikopoulos CV (2016) Heteroaggregation of graphene oxide nanoparticles and kaolinite colloids. EGU General Assembly Conference
- Thio BJ, Zhou D, Keller AA (2011) Influence of natural organic matter on the aggregation and deposition of titanium dioxide nanoparticles. *J Hazard Mater* 189:556–563
- van der Pol E, Coumans FA, Grootemaat AE, Gardiner C, Sargent IL, Harrison P, Sturk A, van Leeuwen TG, Nieuwland R (2014) Particle size distribution of exosomes and microvesicles determined by transmission electron microscopy, flow cytometry, nanoparticle tracking analysis, and resistive pulse sensing. *J Thromb Haemost* 12:1182–1192
- Vasco F, Andrea H, Wim J (2010) Critical evaluation of nanoparticle tracking analysis (NTA) by NanoSight for the measurement of nanoparticles and protein aggregates. *Pharm Res* 27: 796–810
- Xu H, Yang C, Jiang H (2016) Aggregation kinetics of inorganic colloids in eutrophic shallow lakes: influence of cyanobacterial extracellular polymeric substances and electrolyte cations. *Water Res* 106:344–351
- Zhang H, Smith JA, Oyanedel-Craver V (2012) The effect of natural water conditions on the anti-bacterial performance and stability of silver nanoparticles capped with different polymers. *Water Res* 46:691–699
- Zheng Y, Campbell EC, Lucocq J, Riches A, Powis SJ (2013) Monitoring the Rab27 associated exosome pathway using nanoparticle tracking analysis. *Exp Cell Res* 319:1706–1713
- Zhu M, Wang H, Keller AA, Wang T, Li F (2014) The effect of humic acid on the aggregation of titanium dioxide nanoparticles under different pH and ionic strengths. *Sci Total Environ* 487:375–380

Publisher's note Springer Nature remains neutral with regard to jurisdictional claims in published maps and institutional affiliations.